

## ECG-GATED C-ARM COMPUTED TOMOGRAPHY USING L1 REGULARIZATION

Cyril Mory<sup>1,3</sup>, Bo Zhang<sup>3</sup>, Vincent Auvray<sup>3</sup>, Michael Grass<sup>4</sup>, Dirk Schäfer<sup>4</sup>, Françoise Peyrin<sup>1</sup>, Simon Rit<sup>1</sup>,  
Philippe Douek<sup>2</sup>, Loïc Bousset<sup>2</sup>

<sup>1</sup>Université de Lyon, CREATIS ; CNRS UMR5220 ; Inserm U1044 ; INSA-Lyon ; Université Lyon 1, France

<sup>2</sup>Université de Lyon, CREATIS ; CNRS UMR5220 ; Inserm U1044 ; INSA-Lyon ; Université Lyon 1 ; Hospices Civils de Lyon, France

<sup>3</sup>Medisys Research Lab, Philips Healthcare, 33 rue de Verdun, 92156 Suresnes, France

<sup>4</sup>Philips Research Laboratories, Division Technical Systems, Röntgenstrasse 24–26, D-22335 Hamburg, Germany

Phone: +33 4 72 35 74 12, email: cyril.mory@philips.com

### ABSTRACT

*Cardiac C-Arm computed tomography leads to a view-starved reconstruction problem because of electrocardiogram gating. The lack of data has to be compensated by a-priori information on the solution. While standard regularization is performed by minimizing a quadratic penalty term, recently proposed limited-view reconstruction techniques perform it by minimizing the L1-norm of the signal in a basis where it is supposed to be sparse. Although some algorithms are formulated with this generic L1-norm term, their practical implementations replace it by total variation, which leads to piecewise constant images. In this article, we investigate the benefits of using a different sparsifying basis, which can be chosen depending on the expected properties of the solution. It results in more flexibility in the reconstruction. We provide an in-depth description of the algorithm used for the minimization.*

**Index Terms** — C-Arm, computed tomography, ECG-gating, augmented Lagrangian, conjugate gradient

### 1. INTRODUCTION

In the context of acute and chronic coronary artery disease, it would be of great clinical interest to obtain a 4D representation of the myocardium and of the cardiac motion on a C-arm system (in addition to the standard 2D + time coronary angiogram). The main challenge arises from the synchronization with the patient's electrocardiogram (ECG), which is necessary to avoid the motion-induced blurring. Synchronization consists in selecting the projections where the heart is in a given motion state, and discarding all the others. This approach, called "retrospective gating", drastically reduces the number of available projections and creates large gaps in their angular distribution. This leads to an ill-posed reconstruction problem where traditional techniques, such as FBP or ART [1], [2] give disappointing results : the reconstructed images are affected by streak artifacts, which hamper the medical interpretation (see Fig.1).

One way to circumvent the problem is to perform multiple ECG-triggered scan runs around the patient, in order to fill the gaps in the angular sampling[3]. However, with this approach, patients must hold their breath for a long time, get injected a large amount of contrast agent and receive a high radiation dose, so it is often preferred to reconstruct from a single scan run.

Some strategies have been proposed to filter out the streak artifacts from an ECG-gated FBP or ART reconstruction, using deconvolution techniques[4], [5]. They rely on the assumption that the gated reconstruction process is a convolution. This assumption stands in parallel beam geometry only. In fan beam and cone beam geometry, the gated reconstruction process is still linear but no longer stationary (this PSF variation issue is described in [4]), and deconvolution techniques fail.

More promising results were obtained by adding a-priori knowledge in the reconstruction process to restrict the space of solutions. Several limited-view reconstruction techniques based on this idea have been proposed in the last few years [6–8]. These methods minimize a cost function consisting in the sum of a data fidelity term and at least one regularization term. Regularization terms involve the L1 norm of the image in a basis where it is supposed to be sparse. Good results have been obtained using total variation as a sparsifying transform[9], but this tends to generate piecewise constant images.

In this article, we investigate the benefits of using a different sparsifying basis, which can be chosen depending on the expected properties of the solution. It results in more flexibility in the reconstruction. We provide an in-depth description of the algorithm used for the minimization. Preliminary results are presented on a dynamic Shepp-Logan phantom, and on a phantom built from human cardiac CT.

### 2. PROBLEM STATEMENT

Let  $P$  be the ECG-gated forward projection operator,  $p_{\text{measured}}$  the set of ECG-gated measured projections,  $x$  the current reconstructed volume. Let  $W$  be a transform that

sparsifies  $x$ , and  $\sigma$  a real number. We propose to minimize the following cost function:

$$J(x) = \|Px - p_{\text{measured}}\|_2^2 + \sigma \|Wx\|_1$$

This unconstrained problem is equivalent to the following constrained problem:

$$\begin{cases} \text{minimize } K(x, y) = \|Px - p_{\text{measured}}\|_2^2 + \sigma \|y\|_1 \\ \text{subject to } Wx = y \end{cases}$$

We solve this problem by the Augmented Lagrangian[10–12] method, which consists in iteratively minimizing  $K(x, y) + \mu \|Wx - y - d_k\|_2^2$  without constraints, and updating  $d_k$  at each iteration. In the AL method,  $\mu$  is a constant, and  $d_k$  is a term added to control the difference between  $Wx$  and  $y$ .  $d_k$  is initially set to  $d_0 = 0$ .

Minimizing  $K(x, y) + \mu \|Wx - y - d_k\|_2^2$  is done first by finding the  $x$  that minimizes the cost function for a fixed value of  $y$ , then finding the  $y$  that minimizes the cost function for a fixed value of  $x$  (this is the Alternating Direction Method of Multipliers, short ADMM). At each iteration, we compute:

$$\begin{cases} x_{k+1} = \underset{x}{\text{argmin}} \|Px - p_{\text{measured}}\|_2^2 + \mu \|Wx - y_k - d_k\|_2^2 \\ y_{k+1} = \underset{y}{\text{argmin}} \sigma \|y\|_1 + \mu \|Wx_{k+1} - y - d_k\|_2^2 \\ d_{k+1} = d_k - Wx_{k+1} + y_{k+1} \end{cases}$$

### 3. ALGORITHM

#### 3.1. Computing $x_{k+1}$

Computing  $x_{k+1}$  requires minimizing a sum of quadratic forms. The minimum is reached when the gradient of the cost function is zero:

$$\begin{aligned} P^T(Px - p_{\text{measured}}) + \mu W^T(Wx - y_k - d_k) &= 0 \\ \Leftrightarrow (P^T P + \mu W^T W)x &= P^T p_{\text{measured}} + \mu W^T(y_k + d_k) \end{aligned}$$

Note that  $P^T$  is known: it is the unfiltered ECG-gated back projection operator. By defining  $A = P^T P + \mu W^T W$  and  $b = P^T p_{\text{measured}} + \mu W^T(y_k + d_k)$ , we express this problem in its canonical form  $Ax = b$ , and solve it with the conjugate gradient method.

#### 3.2. Computing $y_{k+1}$

The solution to this problem is a soft thresholding of level  $\frac{\sigma}{2\mu}$ :

$$y_{k+1} = ST_{\frac{\sigma}{2\mu}}(Wx_{k+1} - d_k)$$

where  $ST_a(x) = \max(\text{abs}(x) - a, 0) \cdot \text{sign}(x)$ .

#### 3.3. Initialization

The iterative procedure described above requires an initialization. We have tried to use either the ungated FBP or a zero-filled image as a start image. As it could be expected from the results of several other methods that use a prior image [4], [7], [13], we obtained better results using the ungated FBP.

### 4. RESULTS

Preliminary results were obtained using a  $512^2$  pixels modified Shepp-Logan phantom where the fifth ellipse's size varies to simulate a beating heart, and on a real cardiac CT slice that has been animated by an artificial movement vector field. The results have been computed using 600 parallel beam projections, equiangularly distributed in a  $180^\circ$  angular range. Each projection contained 729 rays. This is a rather optimistic, yet realistic setup, as C-Arm CT acquisition protocols typically generate 200 to 600 cone beam projections, equiangularly distributed in a  $180^\circ + \text{fan angle}$  range. The ECG-gating window was a rectangle window of 10% of the cardiac cycle, thus keeping only 60 projections. It was centered alternatively on the point where the ‘‘heart’’ is the biggest (‘End Diastole’) and on the point where it is the smallest (‘End Systole’). The whole experiment was carried out in parallel beam geometry.

Fig.1 displays the results obtained on noiseless data with FBP and three instances of the proposed method, each with its own regularization operator and parameters  $\sigma$  and  $\mu$ :

- in the first one,  $W$  is the gradient,  $\sigma = 0.1$  and  $\mu = 10$
- in the second one,  $W$  is the Haar wavelet decomposition operator with 5 levels of decomposition,  $\sigma = 1$  and  $\mu = 10$
- in the third one,  $W$  is the Daubechies wavelet of order 4 decomposition operator, with 5 levels of decomposition,  $\sigma = 0.1$  and  $\mu = 10$

The exact values of  $\mu$  and  $\sigma$  were determined experimentally, but the rationale is the following:  $\mu$  has to be large enough to constrain  $Wx$  and  $y$  to be approximately equal, otherwise the regularization performed on  $y$  will not affect  $x$ .  $\sigma$  must be chosen so that the soft thresholding operation (which uses  $\frac{\sigma}{2\mu}$  as a threshold) filters out some of the coefficients of  $Wx_{k+1} - d_k$ , but not all of them.

The beating part is pointed out by the arrow. Unlike gated FBP images, images reconstructed with the proposed method contain few streak artifacts. The time resolution can be appreciated by how much the heart in the gated reconstruction matches the one in the phantom. In all three cases, our algorithm clearly provides a better time resolution than the ungated FBP.

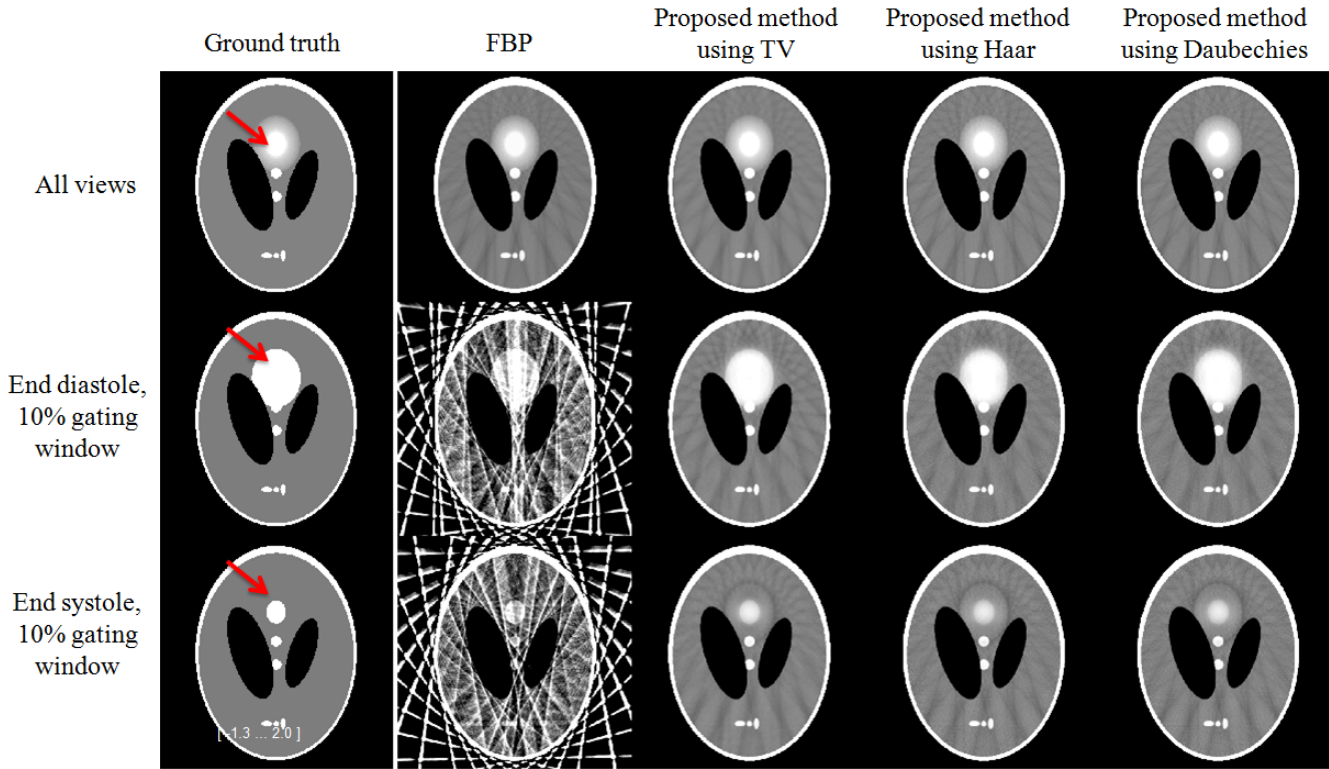


Fig 1. Moving modified Shepp-Logan reconstructions from noiseless data

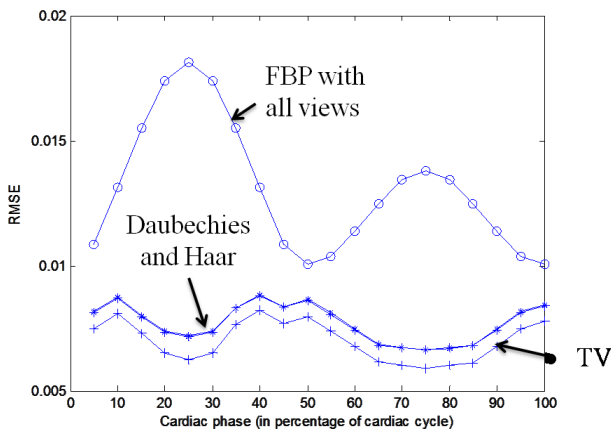


Fig 2. RMSEs measured in the moving area

Fig.2 displays the root mean square error for the FBP with all views, and the proposed method using TV, Haar wavelets and Daubechies wavelets. The RMSE was measured in the moving area only, defined as the area of the heart in end diastole. Note that the curves for Daubechies wavelets and Haar wavelets are too close to be distinguishable. In all three cases, our method clearly reconstructs the area affected by movement with more precision than what can be achieved with FBP. It is also not surprising that TV performs slightly better than wavelets in this case, because the phantom is piecewise constant (and

TV regularization tends to generate piecewise constant images).

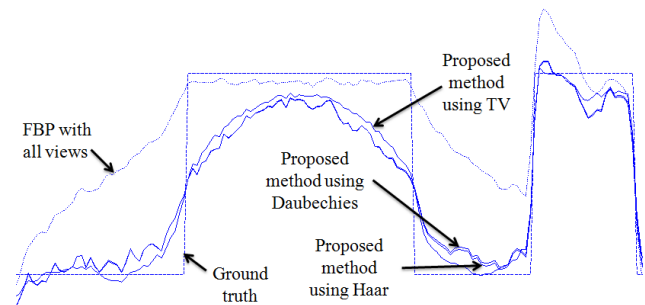


Fig 3. End-systole: profiles in the moving area

Fig.3 shows a profile through the moving area in the reconstructions obtained at end-systole (bottom line of Fig.1), on which the gain in temporal resolution over the FBP with all views is clearly highlighted.

Fig.4 shows the results obtained on noisy data using the exact same reconstruction methods and parameters as for Fig.1. It was simulated by adding to the sinogram a white Gaussian noise of mean 0 and standard deviation 1.5% of the sinogram's dynamic range. Despite the noise, some temporal resolution is still recovered.

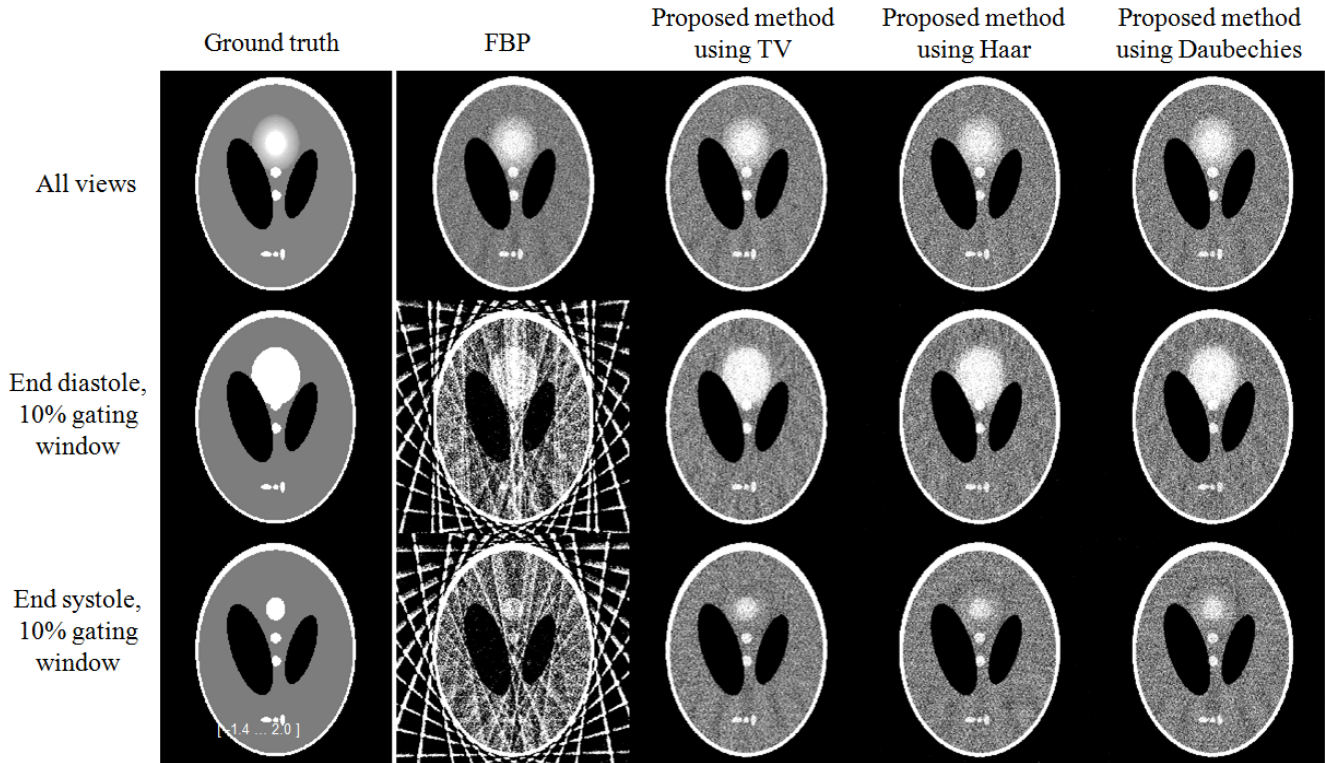


Fig 4. Moving modified Shepp-Logan reconstructions from noisy data

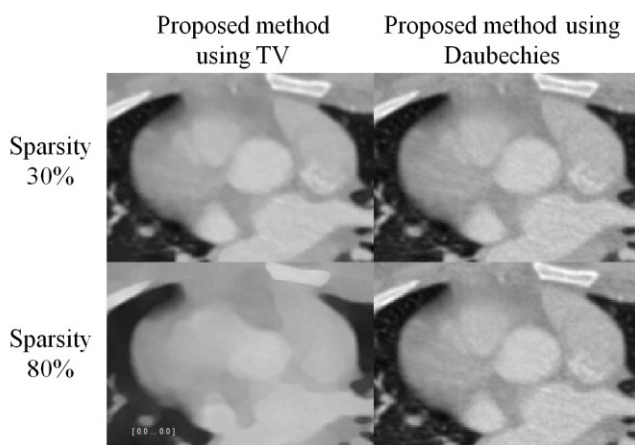


Fig 5. Comparison between regularization with TV and with Daubechies wavelets of order 4

Fig.5 displays the results obtained on a real cardiac CT slice that has been animated by an artificial movement vector field. It shows the difference in texture preservation between TV and wavelet regularization. “Sparsity 30%” means that the parameter  $\sigma$  was set at the first augmented lagrangian iteration so that the soft thresholding sets 30% of the coefficients to zero.  $\sigma$  is then kept unchanged during the rest of the reconstruction. For low levels of regularization, TV and Daubechies wavelets yield similar results. For higher

levels of regularization, Daubechies wavelets preserve the textures better than TV does.

## 5. DISCUSSION

The proposed minimization method requires easy availability of  $W^T$ , which has lead us to consider only Haar and Daubechies wavelets as alternatives to Total Variation, because they are orthogonal, which means that  $W^T = W^{-1}$ . Although it is not shown here, the experiment on the cardiac CT slice also seemed to indicate that a better temporal resolution is achieved using TV. As of now, we do not have any explanation to propose for this phenomenon. The proposed method needs to be applied to real 3D cone beam C-Arm CT data. It should also be compared to state-of-the-art compressed sensing-based methods like PICCS[7].

## 6. CONCLUSION

We have presented and described in details a reconstruction algorithm designed for ECG-gated cardiac C-arm CT, and shown how replacing total variation by another regularization term can lead to improvements in the quality of the reconstruction. The preliminary results are promising. This opens the way to an extensive series of tests aimed at finding the most suitable sparsifying basis for real clinical images.

## 7. REFERENCES

- [1] L. A. Feldkamp, L. C. Davis, and J. W. Kress, "Practical cone-beam algorithm," *J. Opt. Soc. Am. A*, vol. 1, no. 6, pp. 612–619, Jun. 1984.
- [2] A. H. Andersen and A. C. Kak, "Simultaneous algebraic reconstruction technique (SART): a superior implementation of the art algorithm," *Ultrason Imaging*, vol. 6, no. 1, pp. 81–94, Jan. 1984.
- [3] G. Lauritsch, J. Boese, L. Wigström, H. Kemeth, and R. Fahrig, "Towards cardiac C-arm computed tomography," *IEEE Trans Med Imaging*, vol. 25, no. 7, pp. 922–934, Jul. 2006.
- [4] C. T. Badea, S. M. Johnston, Y. Qi, and G. A. Johnson, "4D micro-CT for cardiac and perfusion applications with view under sampling," *Phys. Med. Biol.*, vol. 56, no. 11, pp. 3351–3369, Jun. 2011.
- [5] A. P. Dhawan, R. M. Rangayyan, and R. Gordon, "Image restoration by Wiener deconvolution in limited-view computed tomography," *Appl. Opt.*, vol. 24, no. 23, pp. 4013–4020, décembre 1985.
- [6] E. Y. Sidky and X. Pan, "Image reconstruction in circular cone-beam computed tomography by constrained, total-variation minimization," *Physics in Medicine and Biology*, vol. 53, no. 17, pp. 4777–4807, Sep. 2008.
- [7] G.-H. Chen, J. Tang, and S. Leng, "Prior Image Constrained Compressed Sensing (PICCS)," *Proc Soc Photo Opt Instrum Eng*, vol. 6856, p. 685618, Mar. 2008.
- [8] E. Hansis, D. Schafer, O. Dossel, and M. Grass, "Evaluation of Iterative Sparse Object Reconstruction From Few Projections for 3-D Rotational Coronary Angiography," *IEEE Transactions on Medical Imaging*, vol. 27, no. 11, pp. 1548–1555, Nov. 2008.
- [9] P. T. Lauzier, J. Tang, and G.-H. Chen, "Prior image constrained compressed sensing: Implementation and performance evaluation," *Medical Physics*, vol. 39, no. 1, p. 66, 2012.
- [10] M. Figueiredo, J. M. Bioucas-Dias, and M. V. Afonso, "Fast frame-based image deconvolution using variable splitting and constrained optimization," in *Statistical Signal Processing, 2009. SSP'09. IEEE/SP 15th Workshop on*, 2009, pp. 109–112.
- [11] M. V. Afonso, J. M. Bioucas-Dias, and M. A. T. Figueiredo, "Fast Image Recovery Using Variable Splitting and Constrained Optimization," *Image Processing, IEEE Transactions on*, vol. 19, no. 9, pp. 2345–2356, Sep. 2010.
- [12] M. V. Afonso, J. M. Bioucas-Dias, and M. A. T. Figueiredo, "An Augmented Lagrangian Approach to the Constrained Optimization Formulation of Imaging Inverse Problems," *Image Processing, IEEE Transactions on*, vol. 20, no. 3, pp. 681–695, Mar. 2011.
- [13] G. C. Mc Kinnon and R. H. Bates, "Towards imaging the beating heart usefully with a conventional CT scanner," *IEEE Trans Biomed Eng.*, vol. 28, no. 2, pp. 123–127, Feb. 1981.